von KARMAN INSTITUTE
FOR FLUID DYNAMICS

TECHNICAL NOTE 72

TRAJECTORY READOUT BY PROGRESSIVE ECLIPSING OF A PHOTO - ELECTRIC SCREEN TO OBTAIN AERODYNAMIC FORCE DATA FROM FREE - FLIGHT WIND TUNNEL MODELS

by

P. L. CLEMENS

RHODE-SAINT-GENESE, BELGIUM

MAY 1971

von KARMAN INSTITUTE FOR FLUID DYNAMICS

TECHNICAL NOTE 72

TRAJECTORY READOUT BY PROGRESSIVE ECLIPSING OF A PHOTO - ELECTRIC SCREEN TO OBTAIN AERODYNAMIC FORCE DATA FROM FREE - FLIGHT WIND TUNNEL MODELS

by

P. L. CLEMENS
Visiting Professor
Assistant Manager, Aerospace Instrumentation Branch,
von Karman Gas Dynamics Facility, ARO, Inc.,
Arnold Engineering Development Center, U.S.A.

MAY 1971

ACKNOWLEDGEMENTS

The work with the photo-electric system described in this paper was performed at the von Karman Institute for Fluid Dynamics under the supervision of the author and Prof. K.E. Enkenhus by two students, Messrs L. Six and J. Slechten, as a part of their requirements for the degree "Burgerlijk Elektrotechnisch-Werktuigkundig Ingenieur" earned at the University of Louvain. They are especially to be commended for the enthusiasm and energy with which they pursued their work. The author is indebted also to Messrs J.L. Royen and F. Vande Broeck who operated the VKI Longshot Tunnel during the initial trials with the photo-electrical system and to Prof. B.E. Richards for useful guidance and encouragement given during the course of the work.

ABSTRACT

A newly designed photo-electric system has been used to measure aerodynamic forces on models in the Longshot Wind Tunnel of the von Karman Institute. The system makes use of a periodically interrupted light beam which is progressively eclipsed by the free-flight model. Electronic readout is provided. In early testing, the drag coefficient for a sharp conical model of 9-degree semi-angle has been measured at zero attack angle and at a Mach number of 15 and a Reynolds number of 21×10^6 / meter. The measurement by this method is compared with those from a previously used shadowgraph technique. The latter produces values of drag coefficient either higher (12.9%) or lower (11.1%) depending upon which of two data reduction methods is applied. The value of C_D given by the photo-electric system agrees, within 6.29%, with that given by Talbot's method.

TABLE OF CONTENTS

LIST OF FIGURES

INTRODUCTION

DESIREABILITY AND DISADVANTAGES OF FREE-FLIGHT FORCE TESTING

The advantages of the free-flight measurement of aerodynamic coefficients of force and moment in the wind tunnel are undisputed. Certainly the most direct way of eliminating the effects of support restraint and interference is to eliminate the interfering supports themselves. The shortcomings which are encountered in making such free-flight measurements are found to be associated with the particular measurement techniques used. Care in selecting and in using the techniques is therefore of great importance, lest the shortcomings become overwhelming and the advantages become lost.

Let us consider the disadvantages of the measurement techniques as they are sometimes found in the particular case of a brief duration tunnel having self-luminous flow. Such a case is that of the VKI Longshot Tunnel (ref. 1), in which the vanishing-thread method is used to place a lightweight model in free flight. For the sake of simplicity here, we shall consider that only the aerodynamic coefficient of drag is to be measured. To simplify still further, let us assume that during the useful portion of the tunnel flow (15-20 milliseconds) the density, velocity and angle of attack are all constant, and that the model trajectory is one of pure, streamwise translation in flow having properties which change neither with time nor with distance. (References 1 and 2 treat in detail the variations of method used to treat the less idealized and more practical case.) The equation of motion is, simply:

$$\frac{1}{2}\rho u^2 A C_D = m\frac{d^2x}{dt^2}$$

This may be integrated as:

$$x = q\frac{C_D A}{2m}t^2 + u_0 t + x_0$$

Selecting the origin so as to coincide with the initial displacement term (x_0), the following results:

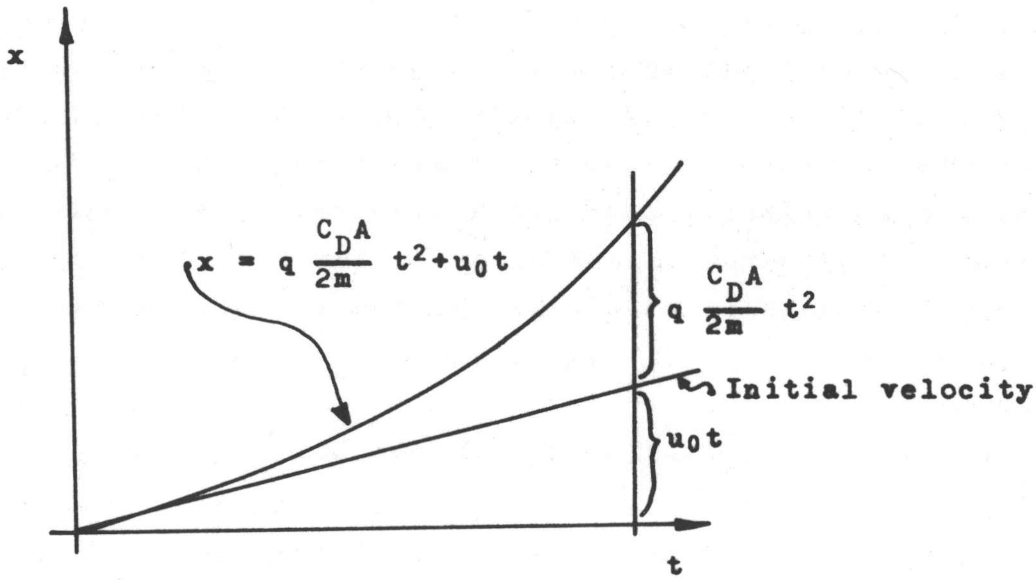

Any of several methods may be used (ref. 2) to arrive at values of the drag coefficient which will best fit a function of this form to the x vs t data actually measured during a particular free-flight test. The drag coefficient may then be evaluated:

$$C_D = \frac{2m}{qAt^2}(x - u_0 t)$$

If only a few data are available to which to fit $x = f(t)$, it is obvious that large errors may appear in C_D. Note especially the manner in which accuracy in C_D depends upon accuracy in the determination of initial velocity, u_0. (Appendix I outlines a somewhat more involved data treatment process for which initial velocity has no direct influence upon the accuracy with which C_D is evaluated).

Photographic techniques ordinarily are employed to gather point-by-point, time-resolved data which enable reconstruction of the model trajectory from which the aerodynamic coefficient is then evaluated by methods of the sort outlined above. Of course, the coefficient can then be determined with no greater accuracy than the photographic recording of trajectory will allow. Because a recording of many well-defined positions of the model is necessary, photography using brief duration exposures and high repetition rates is needed. Fast framing methods (i.e., high-speed ciné-photography) have been used in some past work in the VKI Longshot Tunnel. These fast-framing methods suffer two chief disadvantages: Accuracy suffers owing to frame-to-frame indexing errors, and the small ciné frame size limits spatial resolution, further degrading accuracy. The indexing errors are eliminated if multiple exposures are made on a single stationary negative. Also, since this can be done in large format, improved spatial resolution results.

Large format, multiple-exposure photography has been used in the VKI Longshot Tunnel to record successive positions of the model along its trajectory. This photography has made use of the tunnel's flow visualization system - a conventional, single-pass Toepler schlieren system in the Z configuration. The knife edge is removed from the system, and the viewfield containing the model is illuminated from behind by the repetitive, brief duration spark source. For such a back-lighted, multiple-exposure shadowgraph, the sensitometric properties of the photographic material impose a low limit on the number of silhouette images which can be recorded and then retrieved as data for use in reconstructing the model trajectory. The sketches next page illustrate this. The total exposure given to those areas of the photographic film representing the background comprises the summation of the individual exposures provided by the multi-flash spark source (photographic reciprocity failure and intermittency effects are considered to be negligible in the interest of simplifying the description of the principle involved) and by light "leaks" and self-

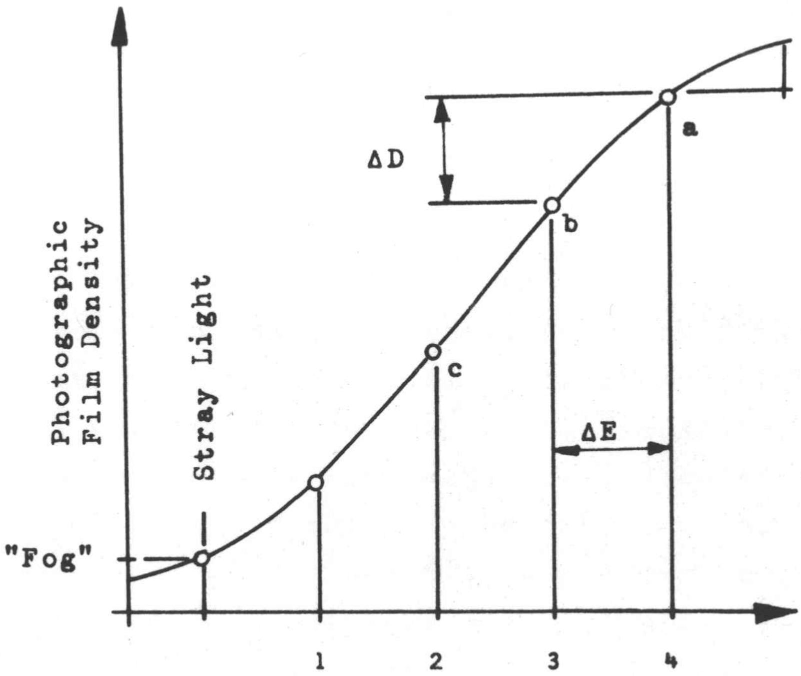

SENSITOMETRIC PLOT

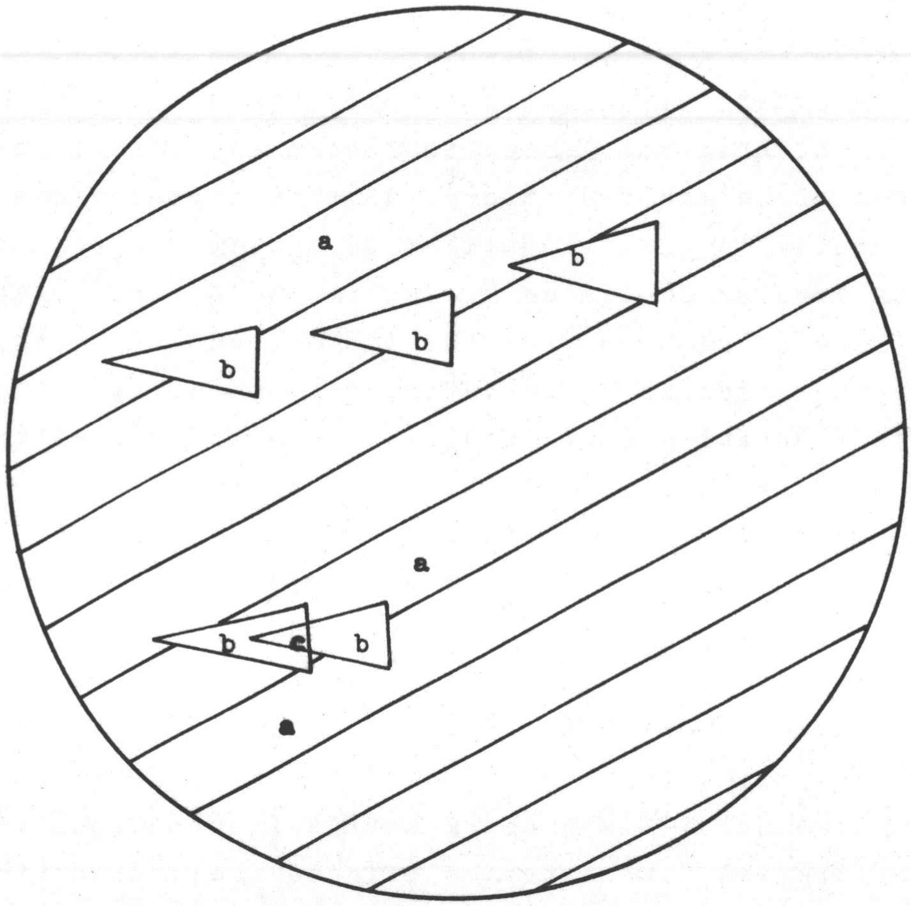

VIEWFIELD

luminosity of the flow. Thus, in the sketch, the background is represented as being exposed to produce the density level shown at point a if four exposures are used. A portion of the film eclipsed by the silhouette image of the model during any one exposure will bear the density level shown at point b. If ΔD represents the least discernable difference in film density, then ΔE must represent the least allowable exposure by a single spark. No more than four exposures can be used in the hypothetical case sketched here. If more than four are used, saturation of the film characteristic is approached, and a less-than-discernable density difference results at the boundary of the model image. If two images overlap, then the photographic density in the region of overlap falls to c. (Overlapping images are common in this work in brief-duration facilities such as the VKI Longshot Tunnel. The overlap results on one hand from the need for high resolution to define the trajectory and, on the other hand, from the small distance travelled during the short period of useful flow by models having ballistic coefficients which are practical. While the short excursion is a handicap to accurate analysis of the trajectory, it is also advantageous to data reduction if, e.g., Mach number distribution is severe or flow angularity or other properties vary in a pronounced way with model position.) However, the zone of density c appears silhouetted against zones of density b rather than a, and no useful contrast advantage greater than ΔD is gained. Thus, it is film latitude which limits the number of trajectory data that can be collected by the use of single-frame back-light photography. Experience with such systems indicates that not many more than ten exposures can be accommodated by ordinary films which are to be interpreted by eye.

This photographic latitude limitation on the number of single-frame trajectory data can be circumvented by front lighting a highly reflective model against a very dark background. If the background is sufficiently non-reflective, it will produce essentially no exposure. If the model is sufficiently reflective, the repetitive source sufficiently intense, and if the photographic optics have sufficiently great light gathering ability, then a satisfactory exposure of the model image will result at each of its successive positions. Eventually, after a very large number of exposures, the photographic density level corresponding to the background will rise intolerably. Rarely does this effect impose any practical limit on the number of exposures, however. Front-light systems of this sort have been used often and with great success in free-flight testing in more conventional, continuous-flow wind tunnels; ref. 3, for example, describes some early work of this kind by Kinslow and Potter in a low-density tunnel at the AEDC. Efforts to adapt the technique to use in the VKI Longshot Tunnel have not been successful. The self-luminous, high-enthalpy flow badly overexposes the film through the large aperture camera lens which must be used with this method. Note that in the case of the back-light system previously described, the lens aperture need be no larger than the image of the spark source; thus self-luminosity of the flow produces much less exposure in that case.

An alternative, photo-electrical trajectory recording method recently has been put to use in the VKI Longshot Tunnel with some success. It produces data providing an essentially continuous description of model position, and it may be used either alone or concurrently with the back-light photographic method. Although only one, drag-measuring channel will be described here, additional channels can be added, e.g., for lift measurement.

PHOTO-ELECTRICAL TRAJECTORY MEASUREMENT

System description

The elements of the photo-electric system appear in fig. 1. A projection system, using a continuously excited incandescent lamp, passes a beam of light which is rectangular in cross section through the tunnel test section. At the tunnel centerline a light screen is thus formed, and the model base intrudes a short distance into this screen as shown in the inset of fig. 1. The portion of the beam not intercepted by the model at the screen position then passes onward to a spherical mirror which brings it to focus in the plane of a toothed rotating chopper wheel. One-hundred, equally-spaced teeth around a balanced aluminum disk of 32-cm. diameter, driven at approximately 3000 rpm, produce a chopping rate of nominally 5 kHz. Beyond the chopper, the beam illuminates the photocathode of a photomultiplier (see circuit diagram, fig. 2). The chopper (fig. 3) permits r-c coupling of the photomultiplier circuit to its readout oscilloscope, reducing "drift". As flow commences, threads supporting the model are abruptly swept away. Model motion then progressively eclipses the rectangular light beam at its screen cross section on the tunnel centerline, diminishing the photmultiplier output signal. Appendix II presents the very simple relationship between output signal and model trajectory and also treats the problems of pitch and yaw interaction.

It would appear that the luminosity of the Longshot Tunnel flow would falsify the photomultiplier signal, just as it produces overexposures of the film during attempts to use the multiple-exposure, front-light photographic system. This is not the case, however. The projection system produces a beam which is quite intense and which is efficiently focussed on the photocathode of the photomultiplier by the second spherical mirror (fig. 1).

Light from the self-luminous flow, on the other hand, is not efficiently brought to focus on the photocathode. This has been verified by removing the projection system and operating the photomultiplier and the chopper during routine operation of the tunnel. The photomultiplier output signal in such cases has been negligible.

The tunnel schlieren system as shown in fig. 1 is arranged for use in the multiple-exposure shadowgraph mode described previously. It functions normally except for the intrusion of the projection system prism into its viewfield.

Static calibration

Static calibration of the photo-electric system is easily carried out using a precision caliper mounted, as in fig. 4, at the position in the tunnel test section later to be occupied by the model. The moveable jaw of the caliper carries an opaque card which is advanced stepwise through the rectangular light screen. Photomultiplier output signal readings are taken from the oscilloscope for each successive position of the opaque card. Figure 5 shows typical calibrations made both before and after a tunnel shot. The discrepancy between the two calibrations shown here resulted from the gradual discharge of the battery used to power the projection lamp. (Use of an improved battery charging and monitoring system has since eliminated discrepancies of this kind.) Variation in illumination intensity over the area of the rectangular screen is responsible for the non-linearity of the calibrations.

Dynamic Calibration

Dynamic calibrations are simply and easily performed by suspending a heavy steel plate in the tunnel test section. The plate, supported on the tunnel centerline from fine wires, hangs initially with its lower edge at the upper extremity of the light screen. The support wires are exploded electrically, allowing the plate to fall freely through the screen in pure translation. Applying the static calibration, the value of gravitational acceleration can be found from the resulting data. (Note that the photo-electric system, e.g., the projection apparatus and photomultiplier, must be rotated through 90° in order to make static calibrations applicable to the case of the dropping plate). In early work with the system, gravitational acceleration values within one percent of the accepted figure were realized repeatedly.

INITIAL RESULTS

In its initial application in the VKI Longshot Tunnel, the photo-electric system described here was used to produce drag data for a sharp-nosed conical model having a 9° semi-angle and tested at a Mach number of 15 and a Reynolds number, per meter, of 21×10^6. Attack angle was zero. A typical data trace appears as fig. 6. Data for comparison were gathered by the multiple-exposure shadowgraph system. Figure 7 shows a typical result from the latter. (The sphere whose silhouette also appears in this six-exposure shadowgraph was a plastic-filled table-tennis ball which was used to produce corrected values of dynamic pressure.)

Reduction of the oscilloscope data produced by the photo-electric system and of the photographic data produced by the shadowgraph system gave the values of drag coefficient shown below. The drag coefficient produced by applying Talbot's method (ref. 4) with data for the viscous interaction parameter from Jones' tables (ref. 5) is also shown for comparison.

Photo-Electrical Method	C_D = 0.0684
Multiple-Exposure Shadowgraph:	
Data reduced by displacement method (see text) .	C_D = 0.0772
Data reduced by curvature method (see App. I) .	C_D = 0.0608
Talbot's Method (ref. 4)	C_D = 0.0641

CONCLUSIONS

The initial test work reported here has shown the photo-electric system to be simply calibrated and easily employed either alone or in conjunction with the multiple-exposure, back-light shadowgraph. It has been shown also to be impervious to flow luminosity. For the particular case of the sharp, slender, conical model used in this work, the drag coefficient produced by the photo-electric system fell between the two values produced by the two different methods of treating the multiple-exposure shadowgraph data which were recorded simultaneously. The value of C_D for the displacement method of shadowgraph data treatment was 12.9 percent higher and that for the curvature method was 11.1 percent lower than the value of C_D given by the photo-electric system. The agreement between the value of C_D from the photo-electric system and that given by Talbot's method was somewhat better: the disparity in this case was 6.29 percent.

The accuracy of the photo-electric system can be defended on the basis of the results of its dynamic calibrations with a freely falling steel plate; the system consistently produced values for gravitational acceleration within one percent of the accepted constant.

REFERENCES

1. RICHARDS, B.E. and ENKENHUS, K.R.: Hypersonic testing in the VKI Longshot Free-Piston Tunnel. AIAA Jnl, vol. 8, No 6, June 1970.

2. ENKENHUS, K.R., CULOTTA, S. and KROGMANN, P.: Free-flight static stability measurements of cones in hypersonic flow. VKI TN 66, 1970.

3. KINSLOW, M. and POTTER, J.L.: The drag of spheres in rarefied hypervelocity flow. AEDC TDR 62-205, December 1962.

4. TALBOT, L., KOGA, T. and SHERMAN, P.: Hypersonic viscous flow over slender cones. NACA TN 4327, 1958.

5. JONES, D.J.: Tables of inviscid supersonic flow about circular cones at incidence $\gamma = 1.4$. AGARDograph 137, November 1969.

APPENDIX I - CURVATURE METHOD OF DATA REDUCTION

The so-called curvature method of data raduction (refs. 1 and 2) is sometimes used in place of the displacement method outlined in the text. In the curvature method, the value of the aerodynamic drag coefficient is assumed to be given by:

$$C_D = K_D C_{Dn} \quad \left[\begin{array}{l} C_{Dn} = \text{Newtonian value of } C_D \\ \\ K_D = \text{constant} \end{array} \right.$$

A theoretical equation of motion can then be written

$$x_{th} = \frac{K_D C_{Dn} A q t^2}{2m} \qquad \text{which assumes } u_0 = 0$$

Assuming the experimental motion to be of the form

$$x_{exp} = \frac{C_D A q t^2}{2m} - u_0 t$$

then

$$\delta_x = x_{exp} - x_{th} = \left(\frac{Aqt^2}{2m}\right) C_D - u_0 t - \left(\frac{Aqt^2}{2m}\right) K_D C_{Dn}$$

$$\delta_x = \frac{Aqt^2}{2m} (C_D - K_D C_{Dn}) - u_0 t$$

The actual value of K_D for which

$$\frac{d^2(\delta_x)}{dt^2} = 0$$

is then taken to produce the desired final value of the drag coefficient. The principle is easily shown graphically:

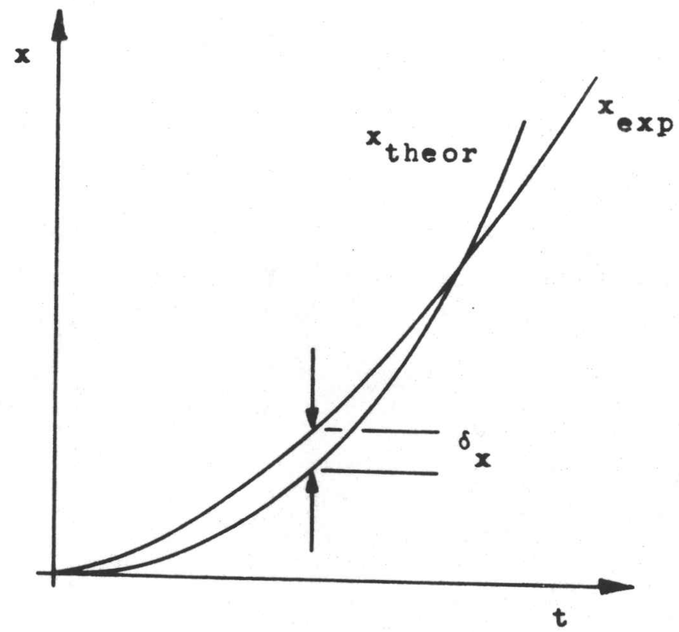

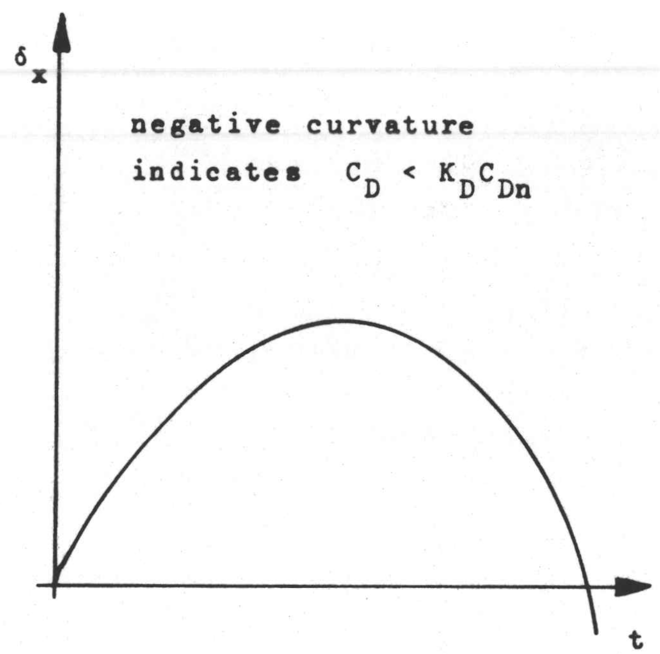

Thus, it is a match in curvature of the model trajectory, irrespective of initial displacement or velocity, which produces the value of drag coefficient.

APPENDIX II - SYSTEM SENSITIVITY AND INTERACTIONS

Assume that the projection system provides uniform illumination throughout a rectangular light screen having vertical dimension _h_, as shown here, with model motion confined to axial translation.

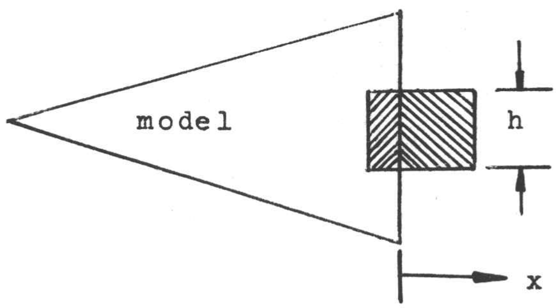

If it is also assumed that the photomultiplier tube responds linearly to photon forcing throughout the range of operation to be used, then

$e_0 = K_c hx$ with e_0 = photomultiplier circuit output signal

$de_0 = K_c h\, dx$ K_c = calibration constant

hence,

$$\frac{de_0}{dt} = K_c h u_0$$

The advantage of increasing the vertical dimension _h_ to produce increased system sensitivity to drag-induced translation is obvious.

Vertical translation of the model, as in response to lift, obviously produces no change in the output signal until the model skirt enters the light screen. Thus if excessive vertical translation is anticipated, the screen dimension _h_ must be compromised against model base diameter. It is obvious too that model roll produces no readout interaction.

Pitch interaction deserves consideration. For this case, the pitch interaction component (see sketch next page) of output signal is:

$$e_{i_0} = K_c(S_1 - S_2)$$

For small angles

$$S_1 \approx \frac{1}{2} h_1^2 \alpha \qquad \text{and}$$

$$S_2 \approx \frac{1}{2} h_2^2 \alpha$$

thence

$$e_{i_0} \approx \frac{K_c}{2} \alpha h(h_1 - h_2)$$

and

$$\frac{de_{i0}}{dt} \approx \frac{K_c}{2} \frac{d\alpha}{dt} h(h_1 - h_2)$$

Several assumptions are convenient in simplifying the case of yaw interaction. Dimensions A and B in the sketches next page are determined by model design. The dimension d represents the extreme to which the model base will have intruded into the light screen as a result of the yaw through angle β.

Since $\qquad A + d = E\cos(\theta - \beta) \qquad$ and $\qquad E = \frac{B}{2\sin\theta}$

then $\qquad d = \frac{B}{2\sin\theta}(\cos\theta\cos\beta + \sin\theta\sin\beta) - A$

$$d = \frac{B}{2}(\cot\theta\cos\beta + \sin\beta) - A$$

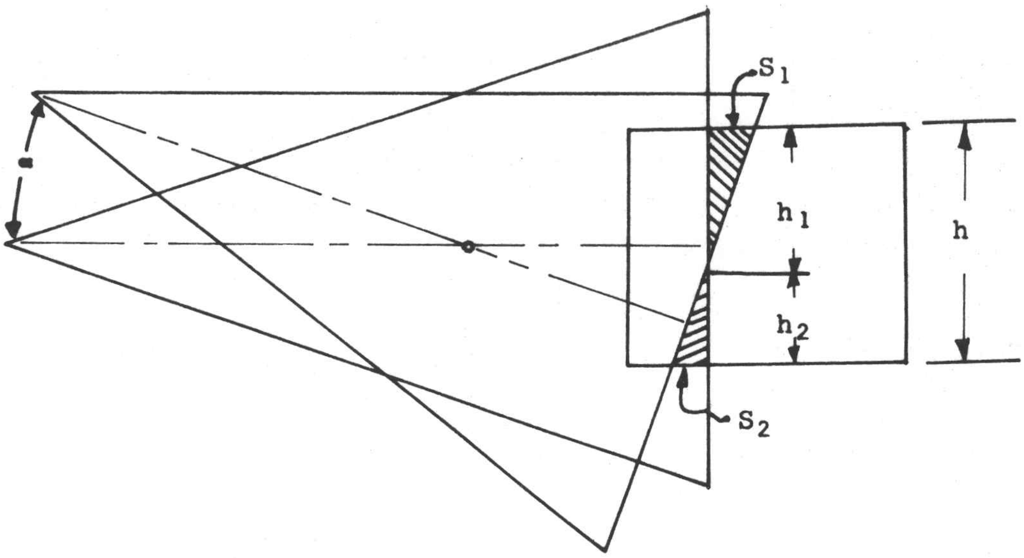

PITCH INTERACTION

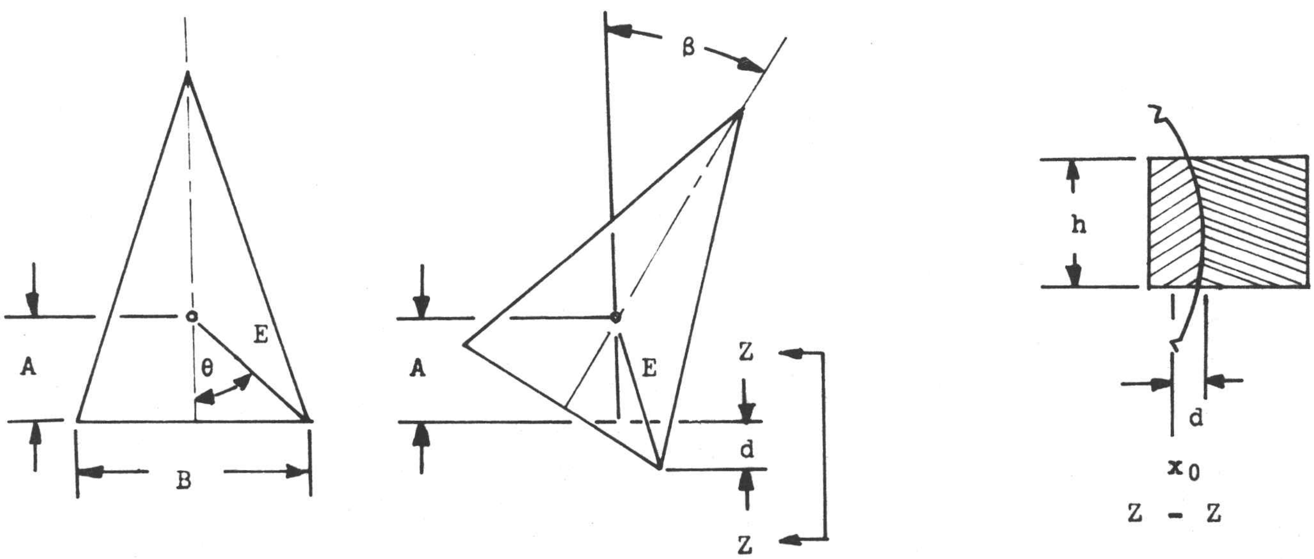

YAW INTERACTION

Making small-angle assumptions $\sin\beta \approx \beta$ and $\cos\beta \approx 1$ and substituting $\frac{2A}{B} = \cot\theta$ produces

$$d \approx \frac{B}{2}\left(\frac{2A}{B} + \beta\right) - A$$

$$d \approx \frac{B}{2}\beta$$

For $B >> h$, then $x \approx d$ (note that this assumption results in the overprediction of yaw interaction) and the yaw interaction component of output signal is

$$e_{i_0} \approx K_c \frac{B}{2}\beta$$

$$\frac{de_{i0}}{dt} \approx K_c \frac{B}{2}\frac{d\beta}{dt}$$

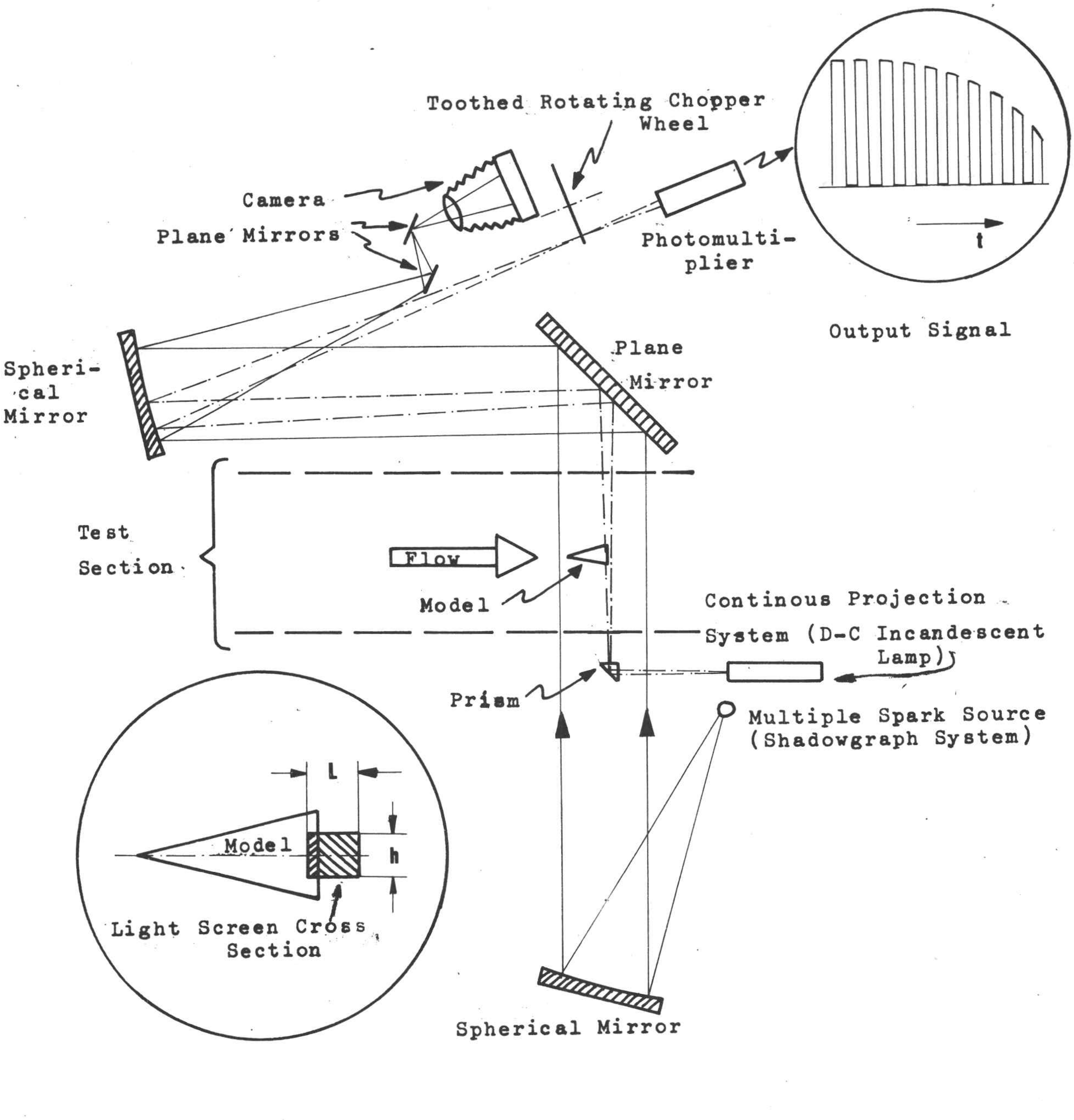

FIG. 1 SHADOWGRAPH AND PHOTO-ELECTRIC SYSTEM

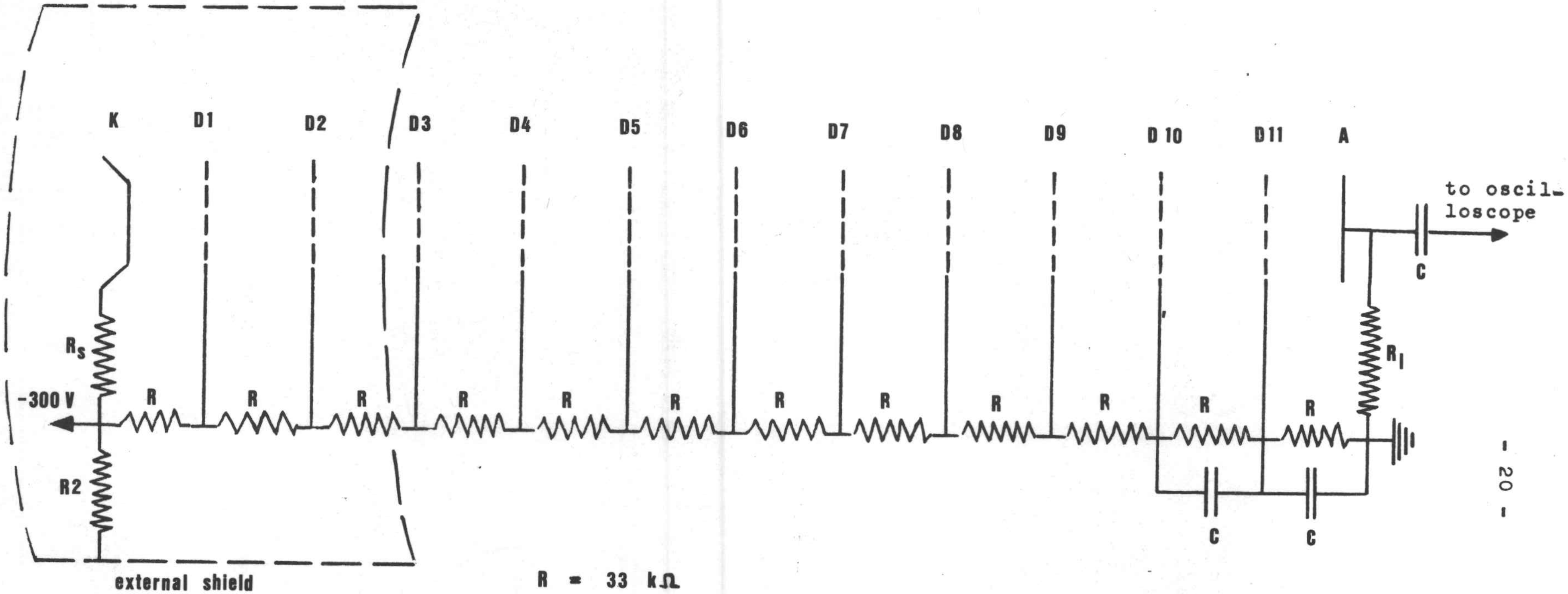

R = 33 kΩ
R_s = 100 kΩ
R_l = 10 kΩ
$R2$ = 10 MΩ
C = 0.1 uF

tube type EMI 9558B

FIG.2 PHOTOMULTIPLIER CIRCUIT

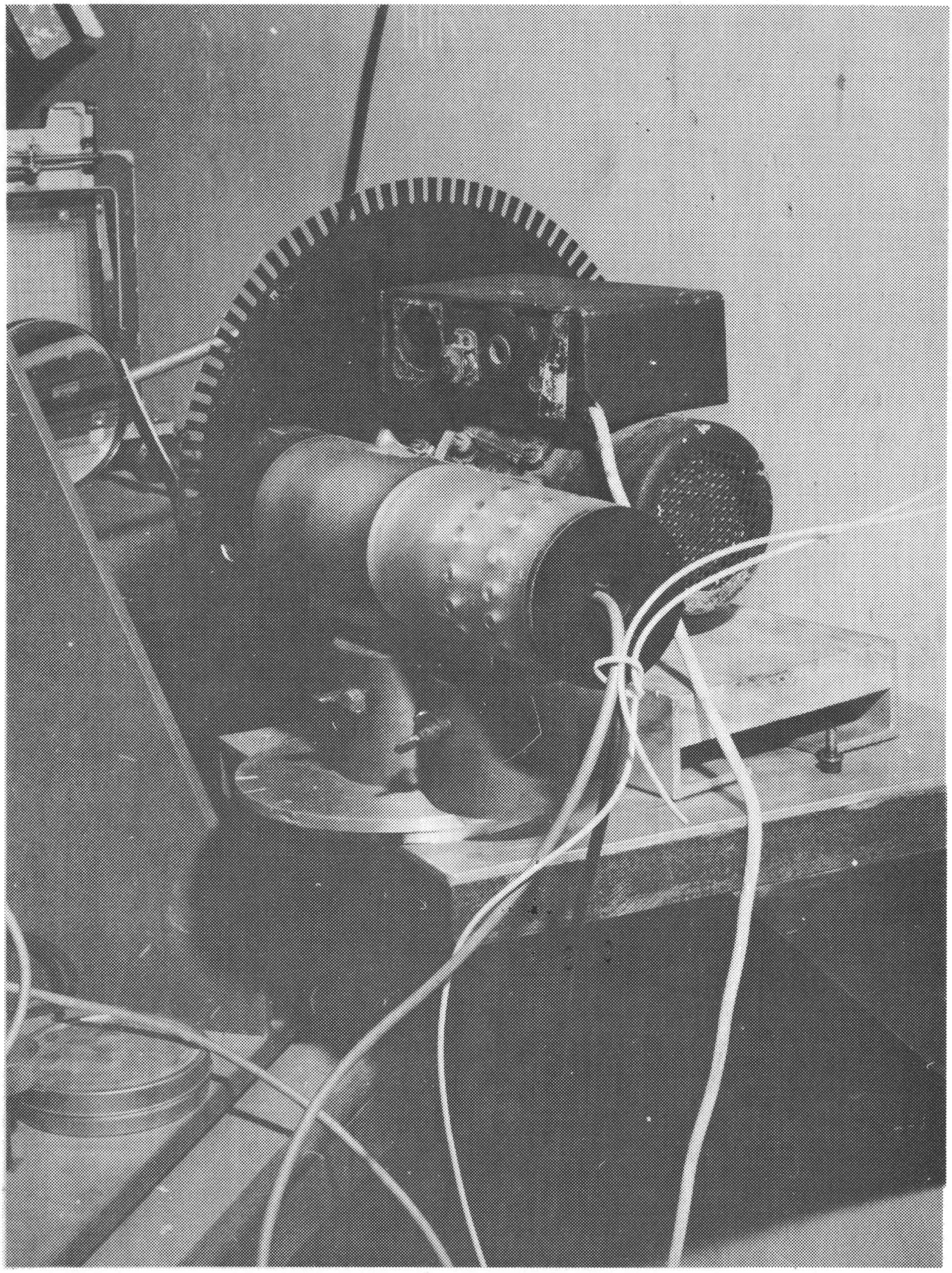

FIG. 3 PHOTOMULTIPLIER WITH CHOPPER

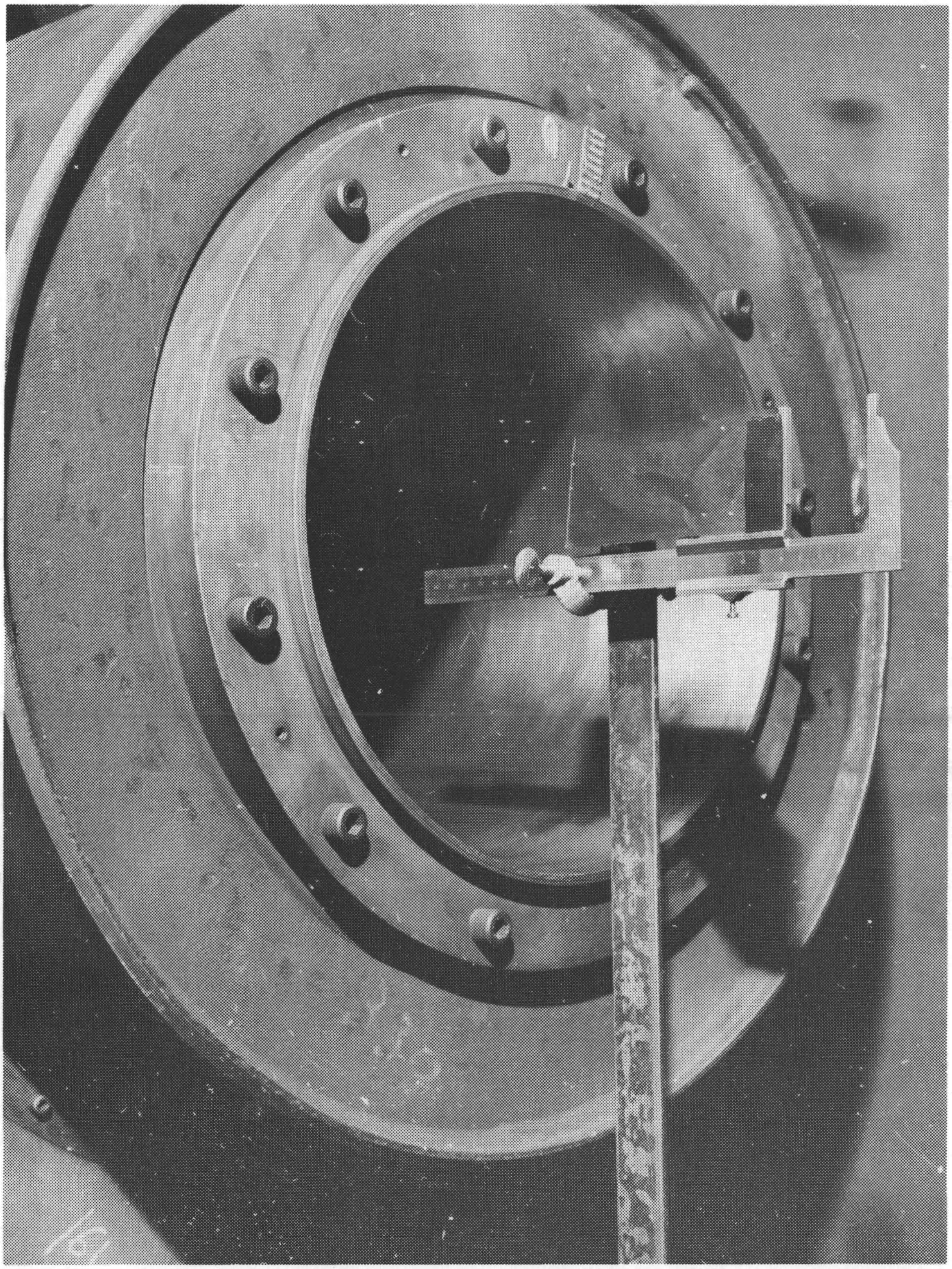

FIG. 4 STATIC CALIBRATION WITH CALIPER

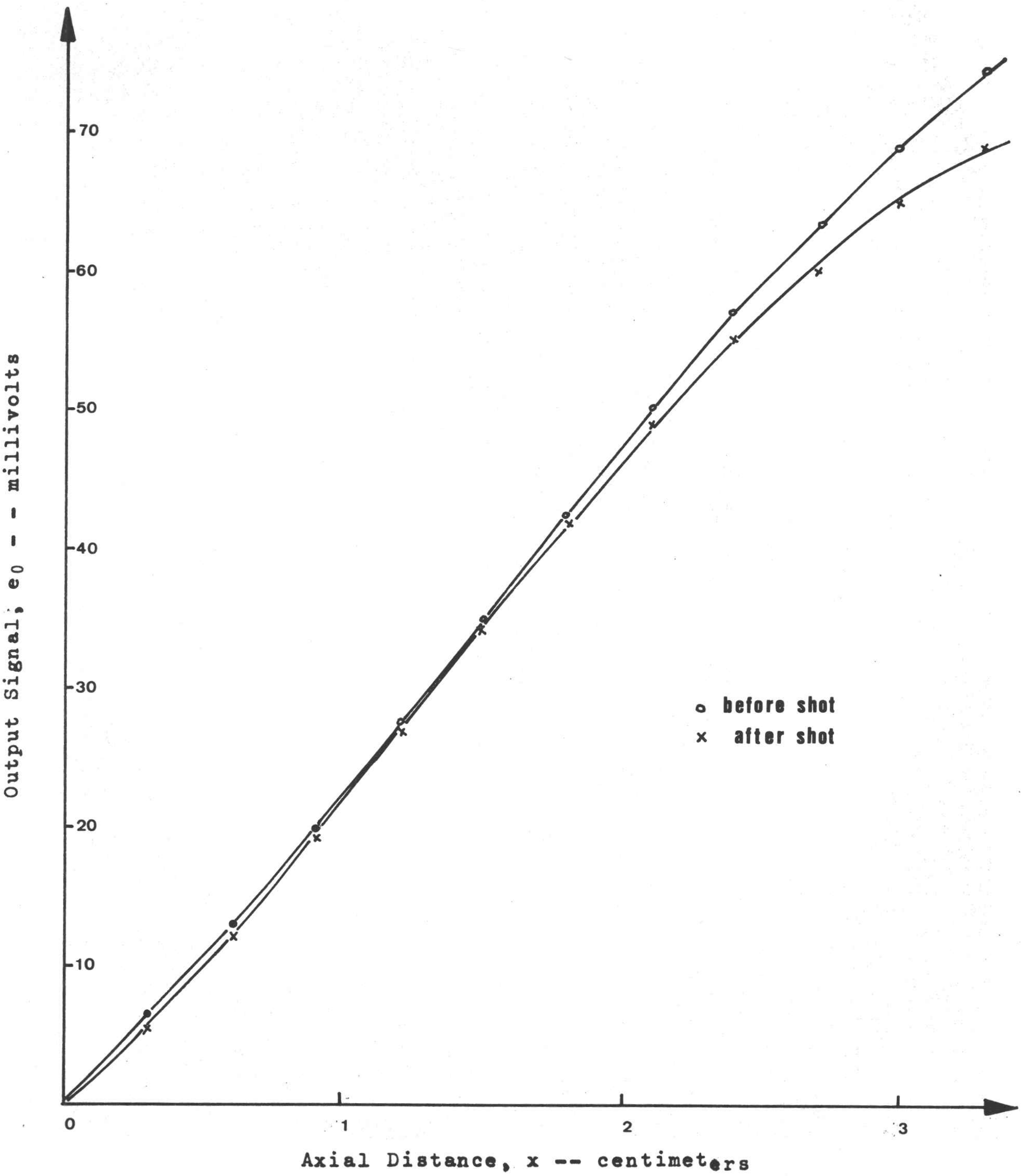

FIG. 5 STATIC CALIBRATION CHARACTERISTIC

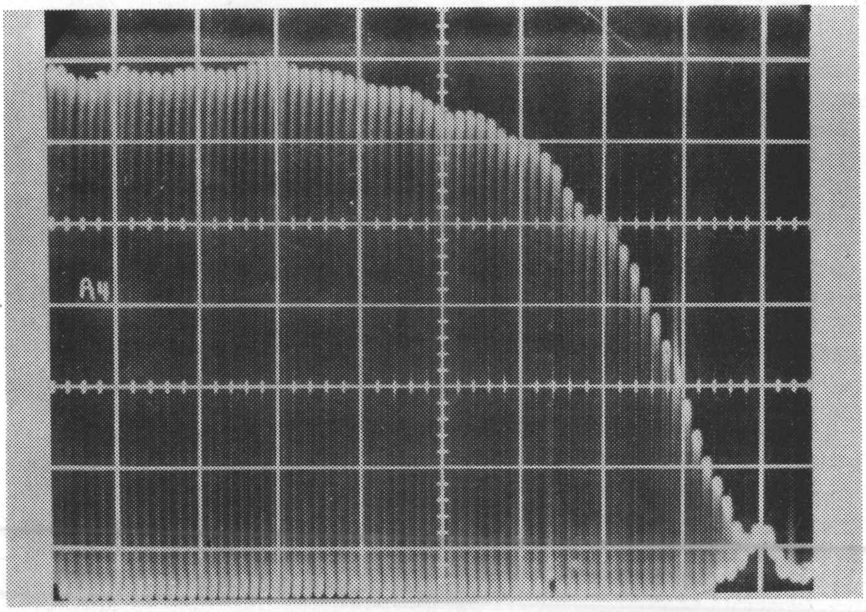

Sweep Rate: 2 millisec/cm.

FIG. 6 OSCILLOSCOPE RECORD FROM PHOTO-ELECTRIC SYSTEM

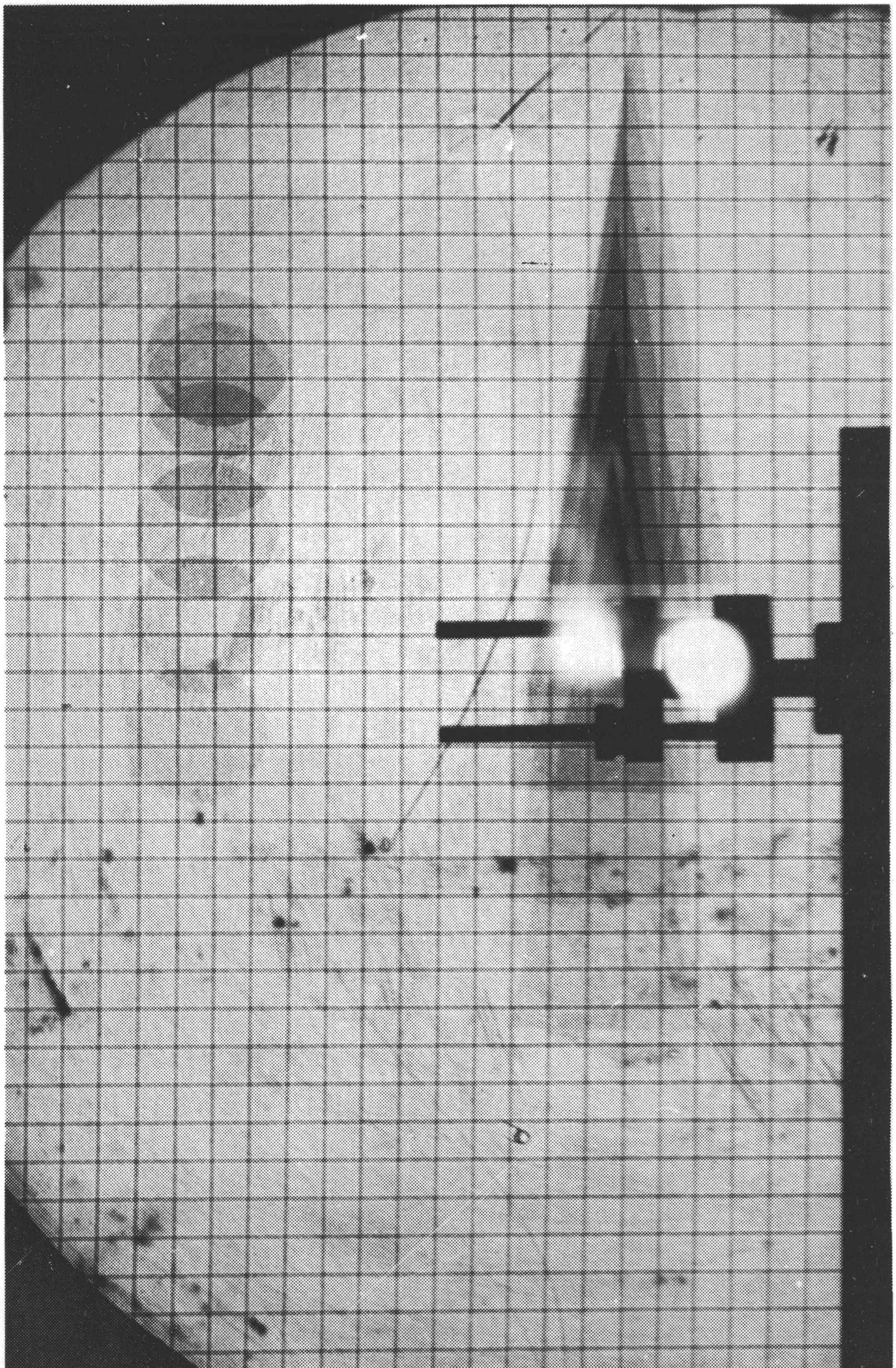

FIG. 7 MULTIPLE-EXPOSURE SHADOWGRAM